



## Extended short-range ferromagnetic order with cluster-glass behavior in Dy<sub>2</sub>AuSi<sub>3</sub>

D.X. Li<sup>a,\*</sup>, S. Nimori<sup>b</sup>, T. Yamamura<sup>c</sup>, K. Yubuta<sup>c</sup>, K. Shirazaki<sup>c</sup>, X. Zhao<sup>a</sup>

<sup>a</sup> Key Laboratory for Anisotropy and Texture of Materials (Ministry of Education), Northeastern University, Shenyang 110004, P.R. China

<sup>b</sup> Tsukuba Magnet Laboratory, National Research Institute for Metals, Tsukuba 305-0003 Japan

<sup>c</sup> Institute for Materials Research, Tohoku University, Oarai, Ibaraki 311-1313 Japan

### ARTICLE INFO

#### Article history:

Received 1 June 2008

Received in revised form 17 October 2008

Accepted 3 November 2008

Available online 17 November 2008

#### Keywords:

Intermetallics

X-ray diffraction

Magnetic measurements

### ABSTRACT

We present the results of ac and dc susceptibilities, high-field magnetization, magnetic relaxation and electrical resistivity measurements for a ternary intermetallic compound Dy<sub>2</sub>AuSi<sub>3</sub> with a hexagonal phase dominant crystal structure derived from the AlB<sub>2</sub>-type. Both the ac and dc susceptibilities show a field and frequency dependent peak around  $T_C \sim 12.5$  K, while evident irreversible magnetism and long-time magnetic relaxation behavior can be observed below  $T_C$ . These metastable magnetic properties suggest that an extended short-range ferromagnetic order occurs near  $T_C$ , i.e. the formation of ferromagnetic cluster state. This is further confirmed by the magnetization and electrical resistivity measurements and by a dynamic analysis of the ac susceptibility data. According to the extended short-range ferromagnetic order model, ferromagnetic clusters in Dy<sub>2</sub>AuSi<sub>3</sub> could exist with larger geometric dimensions, interact magnetically with each other and result in the observed cluster-glass behavior at low temperatures.

© 2008 Elsevier B.V. All rights reserved.

### 1. Introduction

The ternary intermetallic compounds with the general formula R<sub>2</sub>MX<sub>3</sub> (R = rare earth or uranium, M = transition metal, X = Si, Ge, Ga, In) form a large family of compounds, and have been a focus of interest for over 15 years [1,2]. Many of the R<sub>2</sub>TX<sub>3</sub> compounds crystallize in an AlB<sub>2</sub>-derived hexagonal structure (space group *P6/mmm*), which consist of R and M–X layers alternating along the *c*-axis, and the possible crystallographic disorder within M–X positions. These intermetallics exhibit a variety of interesting magnetic properties such as ferromagnetic (FM) ordering in Nd<sub>2</sub>PdSi<sub>3</sub> [3], antiferromagnetic (AFM) ordering in Tb<sub>2</sub>RhSi<sub>3</sub> [4], spin-glass (SG) behavior in U<sub>2</sub>PdSi<sub>3</sub> [5] and Ce<sub>2</sub>AgIn<sub>3</sub> [6], and coexistence of SG state and long-range magnetic order in Dy<sub>2</sub>PdSi<sub>3</sub> [7], Tb<sub>2</sub>PdSi<sub>3</sub> [3,7] and Tb<sub>2</sub>CuIn<sub>3</sub> [8]. A common feature observed for these compounds is the presence of metastable magnetic ground state even for the long-range FM or AFM ordering systems characterized predominantly with the evident difference between field cooling (FC) and zero-field cooling (ZFC) dc susceptibility and long time magnetic relaxation behavior. The formation of SG state in some R<sub>2</sub>TX<sub>3</sub> compounds was attributed to the statistical distribution of the non-magnetic atoms and the latent geometric frustration. Thus these

compounds are also called non-magnetic atom disorder (NMAD) spin glasses.

As a continuation of our studies on the 2:1:3 compounds, we have prepared a polycrystalline Dy<sub>2</sub>AuSi<sub>3</sub> sample and undertaken a systemic measurement on its magnetic properties. In this paper, we present the detailed experimental results including ac susceptibility  $\chi_{ac}(T)$  at different frequencies ( $\omega$ ), high-field magnetization  $M(H)$  up to 110 kOe, FC and ZFC dc susceptibility  $\chi (=M(T)/H)$  in different applied fields  $H$ , magnetic relaxation  $M(t)$  at different temperatures, and electrical resistivity  $\rho(T)$  down to 1.6 K on a well-annealed Dy<sub>2</sub>AuSi<sub>3</sub> sample. To the best of our knowledge, research works on compounds of the R<sub>2</sub>AuSi<sub>3</sub> family with respect to their physical properties were reported only for U<sub>2</sub>AuSi<sub>3</sub> [9] and Ce<sub>2</sub>AuSi<sub>3</sub> [10] up to date.

### 2. Experimental

The polycrystalline sample of Dy<sub>2</sub>AuSi<sub>3</sub> was prepared by melting stoichiometric amounts of the constituent materials in an electric arc furnace under argon atmosphere using four tungsten electrodes and a water-cooled copper hearth. The purities of the materials are Dy: 3N, Au: 4N and Si: 6N. To ensure homogeneity the ingot was remelted several times and annealed at 800 °C for one week in an evacuated quartz tube. X-ray-diffraction measurement was carried out at room temperature with Cu K $\alpha$  radiation to check the purity of the sample. The diffraction patterns reveal that the annealed sample seems to crystallize in a hexagonal phase dominant structure derived from AlB<sub>2</sub>-type with a small amount of a tetragonal impurity phase similar to the compound Ce<sub>2</sub>AuSi<sub>3</sub> after annealing at high temperature [10]. Detailed structural analysis is in progress and will be published elsewhere. The ac susceptibility, dc magnetization and magnetic relaxation were measured using a Quantum Design

\* Corresponding author.

E-mail address: [dxli@imr.tohoku.ac.jp](mailto:dxli@imr.tohoku.ac.jp) (D.X. Li).

superconducting quantum interference device (SQUID) magnetometer. High-field magnetization experiments at 5 K were carried out using an Oxford Instruments VSM 12 T magnetometer in magnetic fields up to 110 kOe, and the absolute value of the magnetization was calibrated using the data measured by a SQUID. Electrical resistivity measurement was performed over temperature range 1.6–280 K using a standard four-terminal method.

### 3. Results and discussion

Fig. 1 shows the temperature dependence of the ZFC dc susceptibility ( $\chi = M/H$ ) and inverse susceptibility of  $\text{Dy}_2\text{AuSi}_3$  measured in an applied field of 100 Oe and in the temperature range 2–300 K. It is clear that the data above 25 K could be nicely fitted using a Curie-Weiss law  $\chi = C/(T - \theta p)$  (dashed line in Fig. 1, right-hand scale), where  $C$  is the Curie constant and  $\theta p$  is the paramagnetic Curie temperature. The best fitting result yields the values of parameter  $C = 4.66 \times 10^{-2}$  emuK/g and  $\theta p = -3.6$  K. From the  $C$  value, an effective magnetic moment  $\mu_{\text{eff}} = 10.63 \mu_{\text{B}}/\text{Dy}$  is obtained, which is very close to the theoretical value expected for a free  $\text{Dy}^{3+}$  ion in the Hund's rule ground state ( $\mu_{\text{eff}} = g\mu_{\text{B}}[J(J+1)]^{1/2} = 10.65 \mu_{\text{B}}$ ) indicating the 4f electrons are almost localized within the Dy atoms. The small negative value of  $\theta p$  indicates the existence of AFM interactions in the sample. This feature is usually observed in typical AFM system and in some magnetic compounds with competitive FM and AFM exchange interactions such as in SG or cluster-glass system. At low temperatures, the susceptibility curve shows a steep rise near  $T_{\text{C}} = 12.5$  K followed by a sharp peak with the peak temperature  $T_{\text{m}} = 11$  K indicating the occurrence of some kind of magnetic phase transition in the  $\text{Dy}_2\text{AuSi}_3$  sample.

In order to get more physical information on the nature of the observed magnetic phase transition around the dc susceptibility peak, ZFC susceptibility is further measured in various applied fields around the transition temperature. As illustrated in Fig. 2, in field strengths up to  $H = 300$  Oe the maximum of the  $\chi_{\text{ZFC}}(T)$  curve increases with rising  $H$ , while the peak position  $T_{\text{m}}$  remains almost unchanged in this field range. With a further increase of applied field the peak of the  $\chi_{\text{ZFC}}(T)$  curve becomes broader and its height decreases, while the  $T_{\text{m}}$  shifts towards lower temperatures. At  $H = 10$  kOe no peak can be observed down to 2 K. These behaviors are characteristic for ferromagnet with domain wall pinning effect [11] or for SG system. Note that although increase of the field strength has an evident influence on the peak position  $T_{\text{m}}$  in fields  $H > 300$  Oe, the kink point  $T_{\text{C}}$  ( $=12.5$  K) of the  $\chi_{\text{ZFC}}$  curve

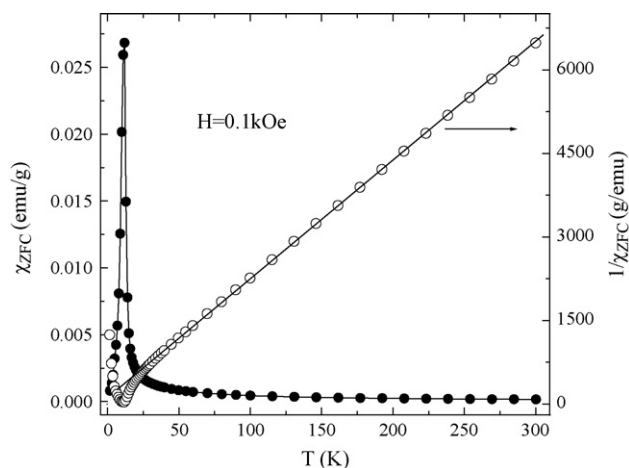


Fig. 1. Temperature dependence of the zero-field cooling dc magnetic susceptibility of  $\text{Dy}_2\text{AuSi}_3$  in a field of 100 Oe, and reciprocal magnetic susceptibility where the solid line represents the fitting result using the Curie-Weiss law in the temperature range between 25 and 300 K.

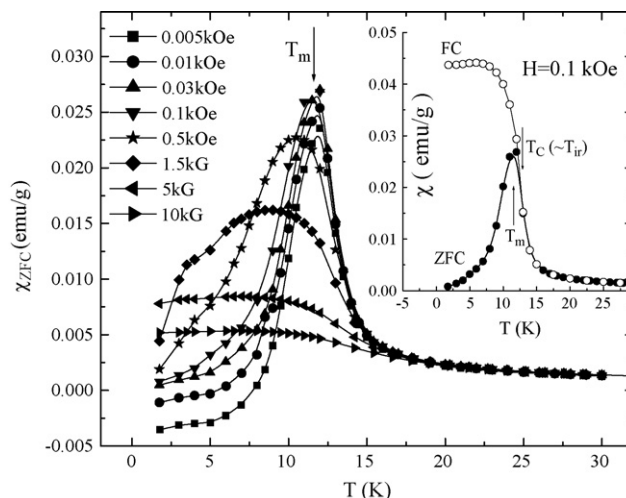
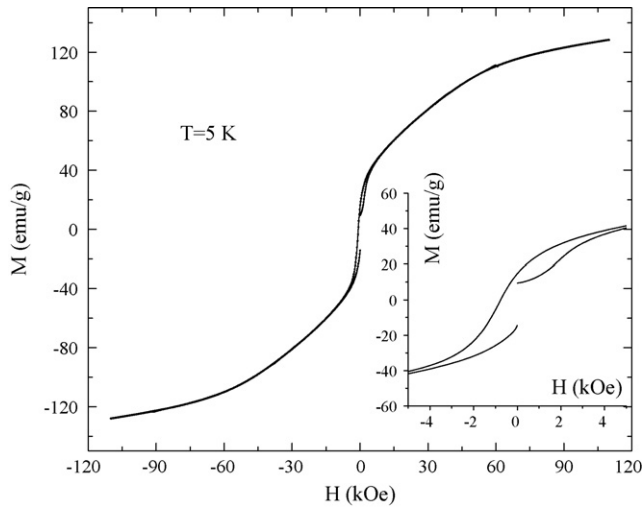


Fig. 2. Temperature dependence of the zero-field cooling dc magnetic susceptibility of  $\text{Dy}_2\text{AuSi}_3$  measured in various applied magnetic fields. The inset shows the difference between the field cooling and zero-field cooling magnetic susceptibilities measured in magnetic field of 100 Oe around the transition temperature.

determined by the minimum of the derivative  $d\chi_{\text{ZFC}}/dT$ , is almost unchanged even rising  $H$  up to 10 kOe. It is interesting to note that the low field ( $<10$  Oe)  $\chi_{\text{ZFC}}$  curve reveals negative magnetic moment at low temperatures. This is because the sample is cooled under a small negative residual field in the superconducting solenoid of the SQUID. This phenomenon can be usually observed for a ferromagnet with high anisotropy and large coercive field [11].

In the inset of Fig. 2, we compare the temperature dependences of FC and ZFC susceptibility measured in a field of 100 Oe for the  $\text{Dy}_2\text{AuSi}_3$  sample. It is clear from this figure that there is no difference between the FC and ZFC curves in the paramagnetic state. With decreasing temperature the magnetic transition peak can be observed only in the  $\chi_{\text{ZFC}}(T)$  curve, while  $\chi_{\text{FC}}(T)$  shows a more rapid rise near the inflection point  $T_{\text{C}}$  and saturation at lower temperatures. This leads to the evident irreversible magnetism manifesting as the bifurcation between the FC and ZFC curves. Note that the irreversibility temperature  $T_{\text{ir}}$  (defined as the temperature below which the  $\chi_{\text{FC}}(T)$  and  $\chi_{\text{ZFC}}(T)$  curve separate from each other) determined at  $H = 100$  Oe is clearly larger than the peak temperature  $T_{\text{m}}$  in  $\chi_{\text{ZFC}}(T)$  curve. This phenomenon is different from that observed for standard SG materials, and can be considered as a characteristic feature for ferromagnet with high magnetic anisotropy or short-range FM order (FM cluster) system. In fact, thermomagnetic irreversibility is a common feature of all magnetic systems with metastable magnetic ground state such as SG, cluster glass and FM materials. In a low field, however, such irreversible magnetism can be observed usually beginning at the peak point  $T_{\text{m}}$  for standard SG and beginning at the inflection temperature  $T_{\text{C}} (>T_{\text{m}})$  for FM cluster or long-range FM ordering system.

Thermodynamically, the observed irreversible magnetism can be directly related to nonequilibrium characters of the low temperature magnetic states, and thus a remanence in hysteresis loop and long time magnetic relaxation effect are also expected at low temperatures for the  $\text{Dy}_2\text{AuSi}_3$  sample. Fig. 3 shows the  $M-H$  curve measured at 5 K ( $<T_{\text{C}}$ ) up to 110 kOe for  $\text{Dy}_2\text{AuSi}_3$ . Though  $M(H)$  shows a tendency to attain the full moment value at high fields, the complete saturation is not achieved in the field range of the measurement. This may be due to the existence of magnetic anisotropy as usually observed in some ferromagnets. With increasing  $H$ ,  $M$  reaches a value of  $128.8$  emu/g ( $=6.99 \mu_{\text{B}}/\text{Dy}$ ) at 110 kOe and when  $H$  is returned from 115 kOe to zero a remanent magnetization of



**Fig. 3.** Magnetization vs. external magnetic field up to 110 kOe for  $\text{Dy}_2\text{AuSi}_3$ . The inset displays the low field part in an expanded scale.

about  $0.8 \mu_B/\text{Dy}$  is detected for the  $\text{Dy}_2\text{AuSi}_3$  sample. From the hysteresis loop we determine the coercive field  $H_C$  of  $\text{Dy}_2\text{AuSi}_3$  to be 760 Oe at 5 K. Moreover, the hysteresis loop shows rapid increase at low fields, this feature is also characteristic for a short-range FM order system.

Fig. 4(a) shows remanent magnetization  $M(t)$  as a function of time  $t$  at several temperatures below  $T_C$ . First, we cooled the sample in zero-field from 50 K (far above  $T_C$ ) to the desired temperature, then a magnetic field of 5 kOe was applied for 5 min and switched off at  $t=0$ . The main finding is that the decay of  $M(t)$  is remarkably slow. After waiting for two hours,  $M(t)$  drops from the initial zero-field value by about 11, 13 and 16% for  $T=5, 7$  and 9 K, respectively. The long time magnetic relaxation behavior is also observed for the  $\text{Dy}_2\text{AuSi}_3$  sample under applied field at temperatures below  $T_C$  (see Fig. 4(b)). Note that the long time magnetic relaxation effect is evident even in a field ( $H=1.5$  kOe) much larger than the coercive field ( $H_C=760$  Oe). This observation is very significant because the long time magnetic relaxation effect in a field  $H$  larger than  $H_C$  is usually considered to originate from the SG state. Thus the present results suggest the possibility of formation of SG (or cluster glass) state

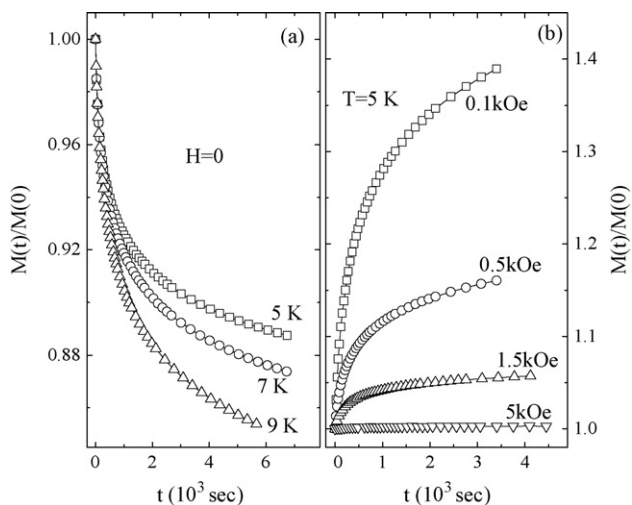


**Fig. 4.** Decay of magnetization measured at 5, 7 and 9 K in zero field (a), and at 5 K in magnetic fields of 0.1, 0.5, 1.5 and 5 kOe (b) for  $\text{Dy}_2\text{AuSi}_3$ , plotted as  $M(t)/M(0)$  vs.  $t$ .

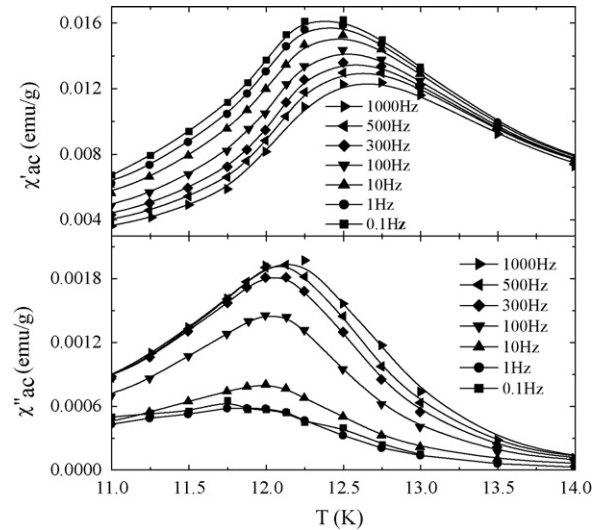


**Fig. 5.** Temperature dependences of real ( $\chi'_{ac}$ ) and imaginary ( $\chi''_{ac}$ ) components of the ac susceptibility of  $\text{Dy}_2\text{AuSi}_3$  measured at various frequencies with an oscillating field of 5 Oe.

in the  $\text{Dy}_2\text{AuSi}_3$  sample at low temperatures. Using a logarithmic function,  $M(t)=M_0-S\ln(t+t_0)$ , the obtained relaxation behaviors shown in Fig. 4(a) and (b) can be fitted very well over the full time range studied with three  $H$ - and  $T$ -dependent fitting parameters: initial zero-field magnetization  $M_0$ , magnetic viscosity  $S$  and characteristic time  $t_0$ .

It is worth emphasizing that the irreversible magnetism and long time magnetic relaxation effect described above are also characteristic of SG materials. In order to get a better insight into the magnetic properties of this compound and to explore the possible SG effect, we have measured the frequency dependence of the real and imaginary parts of the ac susceptibility around the transition temperature. The results at frequency range  $0.1 \text{ Hz} \leq \omega/2\pi \leq 1000 \text{ Hz}$  are illustrated in Fig. 5. It is clear from this figure that the in-phase component of the ac susceptibility,  $\chi'_{ac}$ , exhibits a pronounced maximum at a frequency dependent temperature  $T_C(\omega)$  very close to the inflection point of  $\chi_{ZFC}(T)$  curve shown in Fig. 2. The  $T_C$  value is determined to be 12.36 K at  $\omega/2\pi=0.1$  Hz (in good agreement with the  $T_C$  values shown in Fig. 2), which shifts to 12.62 K at  $\omega/2\pi=1000$  Hz. The upward-shift of the peak position in  $\chi'_{ac}(T)$  curve with rising frequency is a typical feature of SG material, which can be considered as an important evidence for the existence of random spin freezing effect in our  $\text{Dy}_2\text{AuSi}_3$  sample. However, using expression  $\delta T_C = \Delta T_C / (T_C \Delta \log \omega)$ , the frequency shift rate of  $T_C$  is estimated to be  $\delta T_C = 0.005$ . This value is much smaller than the  $\delta T_f$  values (frequency shift rate of freezing temperature) reported for the typical 2:1:3 NMAD SG systems (for examples,  $\delta T_f = 0.022$  for  $\text{Ce}_2\text{AgIn}_3$  [6], 0.016 for  $\text{U}_2\text{PdSi}_3$  [12], 0.015 for  $\text{Nd}_2\text{AgIn}_3$  [13], and 0.016 for  $\text{Ce}_2\text{CuGe}_3$  [14]), but evidently larger than the  $\delta T_m$  values (frequency shift rate of peak temperature) reported for the “almost long range ferromagnetic ordering” compound  $\text{Nd}_2\text{PtSi}_3$  ( $\delta T_f = 0.002$ ) [15]. In this sense, the  $\text{Dy}_2\text{AuSi}_3$  sample could be considered as a FM cluster-glass system, which reveals both FM-like characters (due to the relatively large cluster size) and SG-like behaviors (due to the magnetic exchange interactions between the clusters). The presence of FM cluster-glass effect in  $\text{Dy}_2\text{AuSi}_3$  is further confirmed by a dynamic analysis of the obtained  $T_C(\omega)$  data. We have fitted the  $T_C(\omega)$  data to the standard expression (critical slowing down) [16],  $\tau_{\text{max}} = \tau_0[(T_f - T_s)/T_s]^{-z\nu}$ , and to the Vogel-Fulcher law [17],  $\omega = \omega_0 \exp[-E_a/k_B(T_f - T_{VF})]$ , respectively. Following Tholence [18],  $\tau_0 = 1/\omega_0 = 10^{-13}$  s was kept

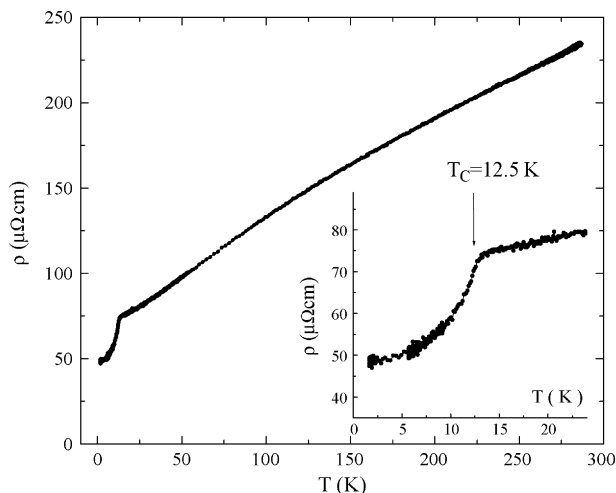


**Fig. 6.** Temperature dependence of the electrical resistivity of  $\text{Dy}_2\text{AuSi}_3$ . The inset shows the data around the transition temperature in an expanded scale.

fixed, the following parameters are obtained from the best fitting results: a static freezing temperature  $T_S = 12.3$  K, a critical (dynamical) exponent  $z\nu = 6.6$ , a Vogel-Fulcher temperature  $T_0 = 11.7$  K and an average activation energy  $E_a \approx 1.75k_B T_S$ . Note that  $z\nu$  is determined around 2 for conventional phase transitions of long-range magnetic ordering systems [19], and around 10 for SG transitions of typical 2:1:3 NMAD SG systems. The  $z\nu$  value obtained for  $\text{Dy}_2\text{AuSi}_3$  in this work is also situated between them. In addition, a characteristic cusp in the imaginary part  $\chi''_{ac}(T)$  and both the peak strength and peak position change significantly with rising frequency are also the indications for cluster glasses or FM systems reflecting different energy losses depending on frequency in the process of phase transition.

On the other hand, another evidence of the presence of large FM cluster in the  $\text{Dy}_2\text{AuSi}_3$  sample is given by the temperature dependence of electrical resistivity measurement. The experimental result is illustrated in Fig. 6. It is seen that the resistivity  $\rho(T)$  reveals metallic conductivity with some negative curvature between 50 and 150 K, which may be resulted from crystal field interaction and/or s-d interband scattering of conduction electrons [20]. As clearly shown in the inset of Fig. 6 in an expanded scale,  $\rho(T)$  curve manifests a sudden bent at  $T_C (=12.5)$ . The rapid decrease of  $\rho$  below  $T_C$  is resulted from the decrease of spin disorder scattering due to FM ordering within the large magnetic clusters. Note that for typical SG systems, no larger anomaly in  $\rho(T)$  curves can be detected.

To summarize, magnetic properties of ternary intermetallic compound  $\text{Dy}_2\text{AuSi}_3$  have been studied by means of ac and dc susceptibility, high-field magnetization, magnetic relaxation, and electrical resistivity measurements. This compound shows a sharp peak in ac and dc susceptibility curves near a transition tempera-

ture  $T_C = 12.5$  K. The upward-shift of the ac susceptibility peak with increasing frequency, the downward-shift of the dc susceptibility peak with increasing magnetic field, the long-time magnetic relaxation behavior and the clear irreversible magnetism below  $T_C$  are observed. In addition, the magnetization measurement measured at 5 K shows a sharp increase at low fields, and electrical resistivity measurement reveals a sudden decrease at  $T_C$ . These features suggest the metastable properties of the magnetic ground state for the  $\text{Dy}_2\text{AuSi}_3$  sample, and can be explained by using an extended short-range FM order model. According to this model, larger FM clusters could exist in the  $\text{Dy}_2\text{AuSi}_3$  sample and magnetic exchange interactions between the clusters occur at low temperature, which leads to the observed FM-like and SG-like features, i.e. FM cluster-glass behaviors. This consequence is further confirmed by a dynamic analysis of the ac susceptibility data, which yields the values of frequency shift rate  $\delta T_C$  and dynamical critical exponent  $z\nu$  being typical for a magnetic cluster system.

## References

- [1] P.A. Kotsanidis, J.K. Yakinthos, E. Gamari-Seale, *J. Magn. Magn. Mater.* 87 (1990) 199.
- [2] R. Pöttgen, D. Kaczorowski, *J. Alloys Compd.* 201 (1993) 157.
- [3] A. Szytula, M. Hofmann, B. Penc, M. Slaski, S. Majumdar, E.V. Sampathkumaran, A. Zygmunt, *J. Magn. Magn. Mater.* 202 (1999) 365.
- [4] A. Szytula, J. Leciejewicz, K. Maletka, *J. Magn. Magn. Mater.* 118 (1993) 302.
- [5] D.X. Li, Y. Shiokawa, Y. Homma, A. Uesawa, A. Dönni, T. Suzuki, Y. Haga, E. Yamamoto, T. Homma, Y. Onuki, *Phys. Rev. B* 57 (1998) 7434.
- [6] T. Nishioka, Y. Tabata, T. Taniguchi, Y. Miyako, *J. Phys. Soc. Jpn.* 69 (2000) 1012.
- [7] D.X. Li, S. Nimori, Y. Shiokawa, Y. Haga, E. Yamamoto, Y. Onuki, *Phys. Rev. B* 68 (2003) 012413.
- [8] I.M. Siouris, I.P. Semitelou, J.K. Yakinthos, W. Schäfer, R.R. Arons, *J. Alloys Compd.* 314 (2001) 1.
- [9] D.X. Li, A. Kimura, Y. Homma, Y. Shiokawa, A. Uesawa, T. Suzuki, *Solid State Commun.* 108 (1998) 863; B. Chevalier, R. Pöttgen, B. Darriet, P. Gravereau, J. Etourneau, *J. Alloys Compd.* 233 (1996) 150.
- [10] R.A. Gordon, C.J. Warren, M.G. Alexander, F.J. DiSalvo, R. Pöttgen, *J. Alloys Compd.* 248 (1997) 24; Subham Majumdar, E.V. Sampathkumaran, *Phys. Rev. B* 62 (2000) 8959.
- [11] T.V. Chandrasekhar Rao, P. Raj, Sk. Mohammad Yusur, L. Madhav Rao, A. Sathyamoorthy, V.C. Sahni, *Philos. Mag. B* 74 (1996) 275.
- [12] D.X. Li, Y. Shiokawa, Y. Haga, E. Yamamoto, Y. Onuki, *J. Phys. Soc. Jpn.* 71 (2002) 418.
- [13] D.X. Li, S. Nimori, Y. Shiokawa, A. Tobo, H. Onodera, Y. Haga, E. Yamamoto, Y. Onuki, *Appl. Phys. Lett.* 79 (2001) 4183.
- [14] C. Tien, C.H. Feng, C. Shui, J.J. Lu, *Phys. Rev. B* 61 (2000) 12151.
- [15] D.X. Li, S. Nimori, Y. Shiokawa, Y. Haga, E. Yamamoto, Y. Onuki, *Solid State Commun.* 120 (2001) 227.
- [16] P.C. Hohenberg, B.I. Halperin, *Rev. Mod. Phys.* 49 (1977) 435; K. Gunnarsson, P. Svedlindh, P. Nordblad, L. Lundgren, H. Aruga, A. Ito, *Phys. Rev. Lett.* 61 (1988) 754.
- [17] H. Vogel, *Phys. Z* 22 (1921) 645; G.S. Fulcher, *J. Am. Ceram. Soc.* 8 (1925) 339.
- [18] J.L. Tholence, *Solid State Commun.* 35 (1980) 113; J.J. Prejean, *J. Phys.* 39 (1978) C6-907; J. Dho, W.S. Kim, N.H. Hur, *Phys. Rev. Lett.* 89 (2002) 27202.
- [19] J.A. Mydosh, *Spin Glass: An Experimental Introduction*, Taylor & Francis, London, 1993.
- [20] D. Kaczorowski, A. Czopnik, W. Suski, V.N. Nikiforov, A.V. Gribanov, *Solid State Commun.* 117 (2001) 373.